Quantum Monte Carlo calculations for light nuclei using chiral forces

Joel Lynn

Theoretical Division, Los Alamos National Laboratory

with

A. Gezerlis, S. Gandolfi, J. Carlson, A. Schwenk, E. Epelbaum

Universality in few-body systems: Theoretical challenges and new directions

Outline

1. Motivation
   - *Ab-initio* calculations for nuclei
   - Nuclear interactions
     - Phenomenology
     - Chiral Effective Field Theory - Standard approach
     - Chiral Effective Field Theory - A new approach
2. Results
   - $A \leq 4$ binding energies
   - $A \leq 4$ radii
   - Perturbative calculations
   - Distributions
3. Conclusion
   - Summary
   - Future work
   - Acknowledgments

Motivation

Ab-initio calculations for nuclei - Quantum Monte Carlo (QMC)

- Nuclear structure methods seek to solve the many-body Schrödinger equation

$$H\left|\Psi\right\rangle = E\left|\Psi\right\rangle .$$

- Variational Monte Carlo (VMC) uses a Metropolis random walk to calculate an upper bound to the ground-state energy:

$$E_T = \frac{\langle\Psi_T|H|\Psi_T\rangle}{\langle\Psi_T|\Psi_T\rangle} \geq E_0.$$

- Green's function Monte Carlo (GFMC) uses propagation in imaginary time to project out the ground state.

$$\left|\Psi(\tau)\right\rangle = e^{-H\tau}\left|\Psi_T\right\rangle \Rightarrow \lim_{\tau\to\infty}\left|\Psi(\tau)\right\rangle \propto \left|\Psi_0\right\rangle .$$

The trial wave function is a symmetrized product of correlation operators acting on a Jastrow wave function.

Trial Wave Function

$$|\Psi_T\rangle = \left[\mathcal{S}\prod_{i<j}(1+U_{ij})\right]|\Psi_J\rangle \,,$$

$$U_{ij} = \sum_{p=2}^{m} u_p(r_{ij})\,O_{ij}^p, \quad |\Psi_J\rangle = \prod_{i<j} f_c(r_{ij})\,|\Phi_A\rangle \,,$$

$$|\Phi_4\rangle = \mathcal{A}\,|p\!\uparrow p\!\downarrow n\!\uparrow n\!\downarrow\rangle \,,$$

$$|\Psi_T\rangle = \left[\mathcal{S}\prod_{i<j}(1+u_\sigma(r_{ij})\boldsymbol{\sigma}_i\cdot\boldsymbol{\sigma}_j + u_{t\tau}(r_{ij})S_{ij}\boldsymbol{\tau}_i\cdot\boldsymbol{\tau}_j)\right]\prod_{i<j} f_c(r_{ij})\,|\Phi_4\rangle$$

GFMC enjoys a reputation as the most accurate method for solving the many-body Schrödinger equation for light nuclei $4 < A \leq 12$.

- First: VMC.
  - We begin with a trial wave function Ψ_T and generate a random position: $\mathbf{R} = \mathbf{r}_1, \mathbf{r}_2, \ldots, \mathbf{r}_A$.
  - Use the Metropolis algorithm to generate new positions $\mathbf{R}'$ based on the probability $P = \frac{|\Psi_T(\mathbf{R}')|^2}{|\Psi_T(\mathbf{R})|^2}$.
  - This gives us a set of "walkers" distributed according to the trial wave function: $\sum_\beta c_\beta \left|\mathbf{R}\beta\right\rangle$. $3A$ positions and $2^A\binom{A}{Z}$ spin/isospin states in the charge basis.

Motivation

Ab-initio calculations for nuclei - QMC

- Second: GFMC.
  - The wave function is imperfect: $\Psi_T = \Psi_0 + \sum_{i\neq 0} c_i \Psi_i$.
  - Propagate in imaginary time to project out the ground state Ψ_0:

$$\Psi(\tau) = e^{-(H-E_T)\tau}\Psi_T = e^{-(E_0-E_T)\tau}\left[\Psi_0 + \sum_{i\neq 0} c_i e^{-(E_i-E_0)\tau}\Psi_i\right]$$

$$\Rightarrow \lim_{\tau\to\infty} \Psi(\tau) \propto \Psi_0.$$

- Second: GFMC.
  The Green's function is calculated by introducing the short-imaginary time $\Delta\tau = \tau/n$.

$$\Psi(\tau) = [\underbrace{e^{-(H-E_T)\Delta\tau}}_{G_{\alpha\beta}(\mathbf{R},\mathbf{R}';\Delta\tau)}]^n \Psi_T$$

$$G_{\alpha\beta}(\mathbf{R},\mathbf{R}';\Delta\tau) = \langle \mathbf{R}\alpha | e^{-(H-E_T)\Delta\tau} | \mathbf{R}'\beta \rangle$$

$$\Psi(\mathbf{R}_n,\tau) = \int d\boldsymbol{\mathcal{R}}\, G(\mathbf{R}_n,\mathbf{R}_{n-1}) \cdots G(\mathbf{R}_1,\mathbf{R}_0)\Psi_T(\mathbf{R}_0)$$

$$d\boldsymbol{\mathcal{R}} = \prod_{i=0}^{n-1} d\mathbf{R}_i$$

- Second: GFMC.
  - We can calculate so-called "mixed estimates":

$$\frac{\langle \Psi(\tau)|O|\Psi_T\rangle}{\langle \Psi(\tau)|\Psi_T\rangle} = \frac{\int d\boldsymbol{\mathcal{R}}\Psi_T^\dagger(\mathbf{R}_n)G^\dagger(\mathbf{R}_n,\mathbf{R}_{n-1})\cdots G^\dagger(\mathbf{R}_1,\mathbf{R}_0)O\Psi_T(\mathbf{R}_0)}{\int d\boldsymbol{\mathcal{R}}\Psi_T^\dagger(\mathbf{R}_n)G^\dagger(\mathbf{R}_n,\mathbf{R}_{n-1})\cdots G^\dagger(\mathbf{R}_1,\mathbf{R}_0)\Psi_T(\mathbf{R}_0)}.$$

$$\langle O(\tau)\rangle = \frac{\langle \Psi(\tau)|O|\Psi(\tau)\rangle}{\langle \Psi(\tau)|\Psi(\tau)\rangle} \approx \langle O(\tau)\rangle_{\text{Mixed}} + [\langle O(\tau)\rangle_{\text{Mixed}} - \langle O\rangle_T].$$

  - For ground-state energies, $O = H$, and $[H, G] = 0$:

$$\langle H\rangle_{\text{Mixed}} = \frac{\langle \Psi_T|e^{-(H-E_T)\tau/2}He^{-(H-E_T)\tau/2}|\Psi_T\rangle}{\langle \Psi_T|e^{-(H-E_T)\tau/2}e^{-(H-E_T)\tau/2}|\Psi_T\rangle}$$

$$\lim_{\tau\to\infty}\langle H\rangle_{\text{Mixed}} = E_0.$$

- A fundamental goal of low-energy nuclear physics is to describe and calculate properties of nuclei in terms of realistic bare nuclear interactions.
- Quantum chromodynamics (QCD) is the underlying theory, but nucleons are the relevant degrees of freedom for low-energy nuclear physics → nucleon-nucleon potentials.

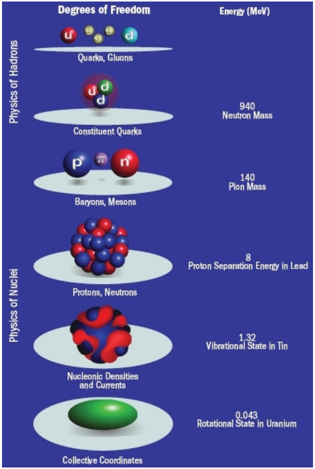

Figure 1: From www.scidacreview.org

Motivation

Nuclear interactions - The Hamiltonian

$$H = \sum_{i=1}^{A} \frac{\mathbf{p}_i^2}{2m_i} + \sum_{i<j}^{A} v_{ij} + \sum_{i<j<k}^{A} V_{ijk} + \cdots$$

The focus of this talk is on the two-body interaction. Until now, there were two broad choices for v_{ij}.

- Local, real-space, phenomenological: Argonne's v_{18}[1] - informed by theory, phenomenology, and experiment (well tested and very successful).
- Non-local, momentum-space, effective field theory (EFT): $\mathrm{N^3LO}$[2] - informed by chiral EFT and experiment (well liked and often used in basis-set methods, such as the no-core shell model).

[1] R. B. Wiringa, V. G. J. Stoks, and R. Schiavilla, Phys. Rev. C **51**, 38 (1995).

[2] e.g. D. R. Entem and R. Machleidt, Phys. Rev. C **68**, 041001 (2003)

Argonne's v_{18} consists of three parts.

$$v_{ij} = v_{ij}^{\gamma} + v_{ij}^{\pi} + v_{ij}^{R}.$$

- v_{ij}^{γ} includes one- and two-photon exchange Coulomb interactions, vacuum polarization, Darwin-Foldy, and magnetic moment terms with appropriate proton and neutron form factors.
- v_{ij}^{π} includes charge-dependent terms due to the difference in neutral and charged pion masses.
- v_{ij}^{R} is a short-range phenomenological potential.

Motivation

Nuclear interactions - Argonne's v_{18}

Operator form

$$v_{ij}^{\pi} + v_{ij}^{R} = \sum_{p=1}^{18} v_p(r_{ij})\, O_{ij}^{p}.$$

Charge-independent operators

$$O_{ij}^{p=1,14} = \left[1, \boldsymbol{\sigma}_i \cdot \boldsymbol{\sigma}_j, S_{ij}, \mathbf{L}\cdot\mathbf{S}, \mathbf{L}^2, \mathbf{L}^2(\boldsymbol{\sigma}_i \cdot \boldsymbol{\sigma}_j), (\mathbf{L}\cdot\mathbf{S})^2\right] \otimes [1, \boldsymbol{\tau}_i \cdot \boldsymbol{\tau}_j].$$

Charge-independence-breaking operators

$$O_{ij}^{p=15,18} = [1, \boldsymbol{\sigma}_i \cdot \boldsymbol{\sigma}_j, S_{ij}] \otimes T_{ij}, \text{ and } (\tau_{zi} + \tau_{zj}).$$

Tensor operators

$$S_{ij} = 3(\boldsymbol{\sigma}_i \cdot \hat{\mathbf{r}}_{ij})(\boldsymbol{\sigma}_j \cdot \hat{\mathbf{r}}_{ij}) - \boldsymbol{\sigma}_i \cdot \boldsymbol{\sigma}_j,\; T_{ij} = 3\tau_{zi}\tau_{zj} - \boldsymbol{\tau}_i \cdot \boldsymbol{\tau}_j$$

Motivation

Nuclear interactions - Argonne's v_{18}

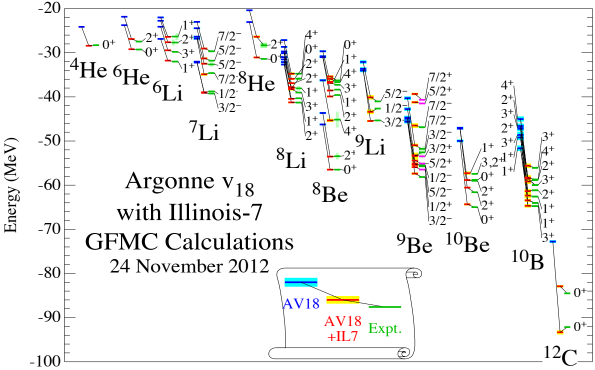

Figure 2: Many excellent results using Green's function Monte Carlo (GFMC) and phenomenological potentials. From http://www.phy.anl.gov/theory.

This is great! But... Until now the nucleon-nucleon potentials used have been restricted to the phenomenological Argonne-Urbana/Illinois family of interactions.

Chiral EFT makes a more direct connection between QCD and the nuclear force.

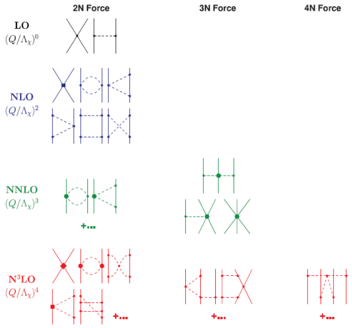

Figure 3: Hierarchy of the nuclear force in chiral EFT, from R. Machleidt and D. Entem, Phys. Rep. **503**, 1 (2011).

Weinberg prescription

- Start from the most general Lagrangian consistent with all symmetries of the underlying interaction...
  $\mathcal{L} = \mathcal{L}_{\pi\pi} + \mathcal{L}_{\pi N} + \mathcal{L}_{NN} + \cdots$
- Define a power-counting scheme...
  $\nu = -4+2N+2L+\sum_i V_i\Delta_i,$
  $\Delta_i = d_i + \frac{1}{2}n_i - 2.$

Chiral EFT makes a more direct connection between QCD and the nuclear force.

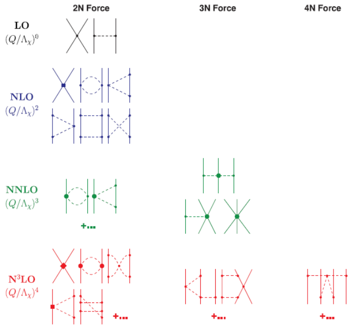

Figure 3: Hierarchy of the nuclear force in chiral EFT, from R. Machleidt and D. Entem, Phys. Rep. **503**, 1 (2011).

Weinberg prescription

- An expansion in (Q/Λ_χ).
- Q is a soft momentum scale.
- $\Lambda_\chi \sim 1$ GeV is the chiral-symmetry-breaking scale.

For example, the leading-order (LO) diagrams lead to

$$V_{NN}^{(0)} \propto \frac{(\boldsymbol{\sigma}_1 \cdot \mathbf{q})(\boldsymbol{\sigma}_2 \cdot \mathbf{q})}{\mathbf{q}^2 + M_\pi^2} \boldsymbol{\tau}_1 \cdot \boldsymbol{\tau}_2 + \cdots$$

Chiral EFT makes a more direct connection between QCD and the nuclear force.

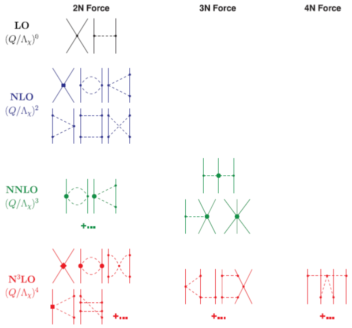

Figure 3: Hierarchy of the nuclear force in chiral EFT, from R. Machleidt and D. Entem, Phys. Rep. **503**, 1 (2011).

Sources of non-locality in standard approach[a] [b]

- Regulator: $f(p, p') = e^{-(p/\Lambda)^n} e^{-(p'/\Lambda)^n}$.
- Contact interactions $\propto \mathbf{k} = (\mathbf{p} + \mathbf{p}')/2$.

$\mathcal{F}[V(\mathbf{p}, \mathbf{p}')] \to V(\mathbf{r}, \mathbf{r}')$.

---

[a] D. Entem and R. Machleidt, Phys. Rev. C **68**, 041001 (2003)

[b] E. Epelbaum, W.Glöckle and U.-G. Meißner, Eur. Phys. J. A **19**, 401 (2004)

Chiral EFT makes a more direct connection between QCD and the nuclear force.

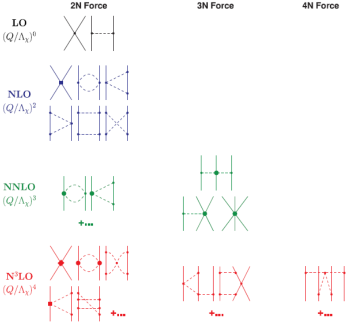

Figure 3: Hierarchy of the nuclear force in chiral EFT, from R. Machleidt and D. Entem, Phys. Rep. **503**, 1 (2011).

New approach[a]

- Regulator: $f_{\text{long}}(r) = 1 - e^{-(r/R_0)^4}$.
- Up to N^{2}LO, $V_\pi = V_\pi(\mathbf{q})$, $\mathbf{q} = \mathbf{p}' - \mathbf{p}$.
- Antisymmetry allows for the selection of contacts not proportional to $\mathbf{k}$ (almost).

$\mathcal{F}[V(\mathbf{q})] \to V(\mathbf{r})$
$\Rightarrow$ Local!

[a] A. Gezerlis et al., Phys. Rev. Lett. **111**, 032501 (2013)

Chiral EFT makes a more direct connection between QCD and the nuclear force.

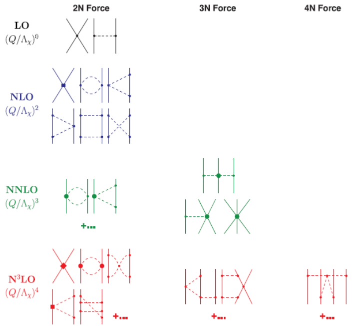

Figure 3: Hierarchy of the nuclear force in chiral EFT, from R. Machleidt and D. Entem, Phys. Rep. **503**, 1 (2011).

New approach[a]

$$V(r) = V_C(r) + W_C(r)\boldsymbol{\tau}_1 \cdot \boldsymbol{\tau}_2$$
$$+ (V_S(r) + W_S(r)\boldsymbol{\tau}_1 \cdot \boldsymbol{\tau}_2)\boldsymbol{\sigma}_1 \cdot \boldsymbol{\sigma}_2$$
$$+ (V_T(r) + W_T(r)\boldsymbol{\tau}_1 \cdot \boldsymbol{\tau}_2)S_{12}.$$

$$V_C(r) =$$
$$\frac{1}{2\pi^2 r}\int_{2M_\pi}^{\tilde{\Lambda}} d\mu \mu e^{-\mu r}\rho_C(\mu), \text{ etc.}$$

[a] A. Gezerlis et al., Phys. Rev. Lett. **111**, 032501 (2013)

Local chiral EFT potential $\sim$ a v_7 potential

$$v_{ij} = \sum_{p=1}^{7} v_p(r_{ij})\, O_{ij}^p + \sum_{p=15}^{18} v_p(r_{ij})\, O_{ij}^p.$$

Charge-independent operators

$$O_{ij}^{p=1,14} = \left[1, \boldsymbol{\sigma}_i \cdot \boldsymbol{\sigma}_j, S_{ij}, \mathbf{L}\cdot\mathbf{S}, \mathbf{L}^2, \mathbf{L}^2(\boldsymbol{\sigma}_i \cdot \boldsymbol{\sigma}_j), (\mathbf{L}\cdot\mathbf{S})^2\right] \otimes [1, \boldsymbol{\tau}_i \cdot \boldsymbol{\tau}_j]\,.$$

Charge-independence-breaking operators

$$O_{ij}^{p=15,18} = [1, \boldsymbol{\sigma}_i \cdot \boldsymbol{\sigma}_j, S_{ij}] \otimes T_{ij},\ \text{and}\ (\tau_{zi} + \tau_{zj}).$$

Tensor operators

$$S_{ij} = 3(\boldsymbol{\sigma}_i \cdot \hat{\mathbf{r}}_{ij})(\boldsymbol{\sigma}_j \cdot \hat{\mathbf{r}}_{ij}) - \boldsymbol{\sigma}_i \cdot \boldsymbol{\sigma}_j,\ T_{ij} = 3\tau_{zi}\tau_{zj} - \boldsymbol{\tau}_i \cdot \boldsymbol{\tau}_j$$

Motivation

Nuclear interactions - Chiral EFT

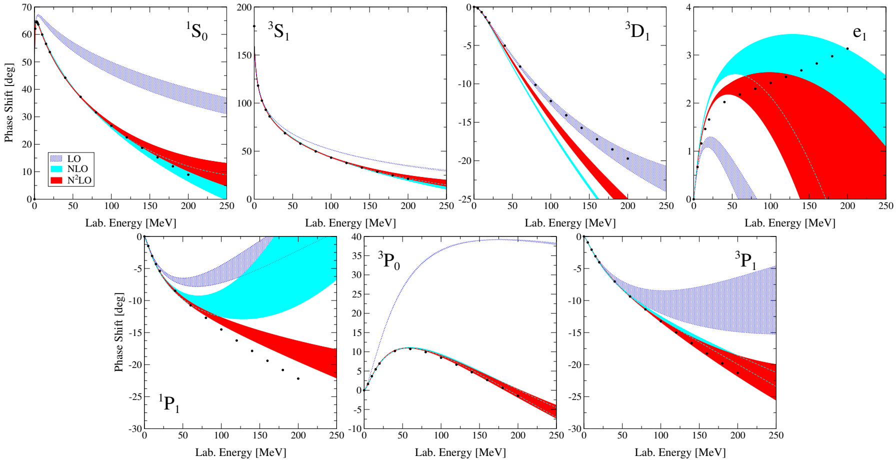

Figure 4: (PRELIMINARY) Phase shifts for the *np* potential. From A. Gezerlis et al. in preparation.

Results

^{2}H binding energies - $\langle H \rangle$

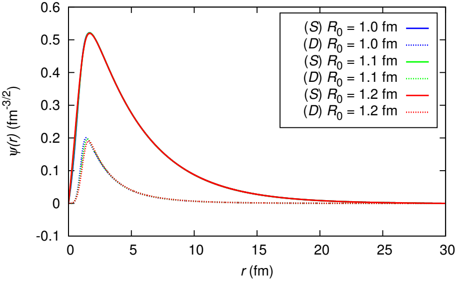

Figure 5: Deuteron wave functions at N^{2}LO.

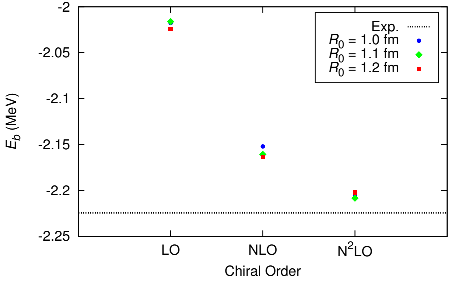

Figure 6: ^{2}H binding energy at different chiral orders and cutoff values.

Results

$A = 3$ binding energies - $\langle H \rangle$

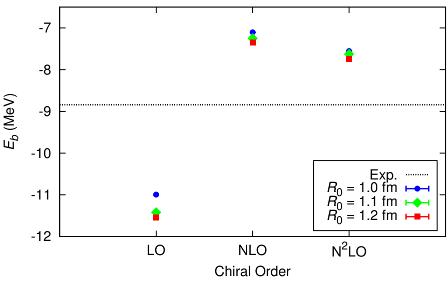

Figure 7: ^{3}H binding energy at different chiral orders and cutoff values.

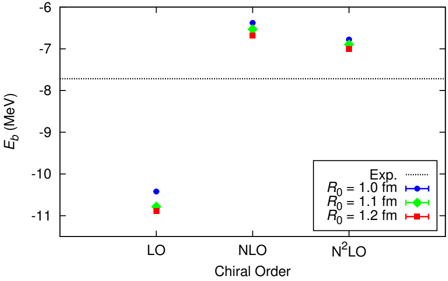

Figure 8: ^{3}He binding energy at different chiral orders and cutoff values.

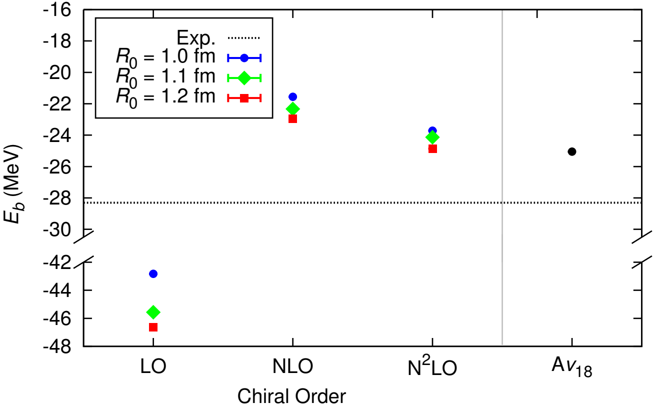

Figure 9: ^{4}He binding energy at different chiral orders and cutoff values.

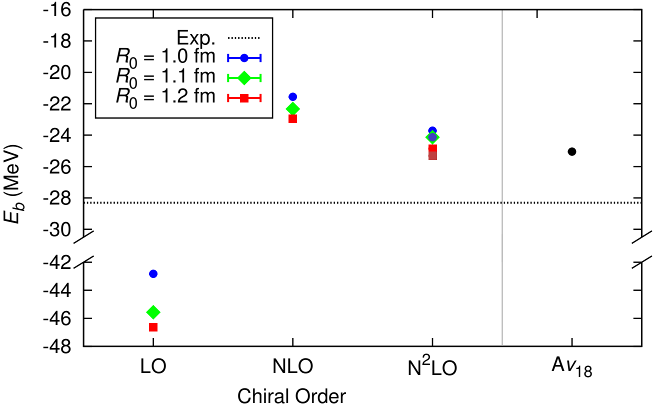

Figure 9: ^{4}He binding energy at different chiral orders and cutoff values.

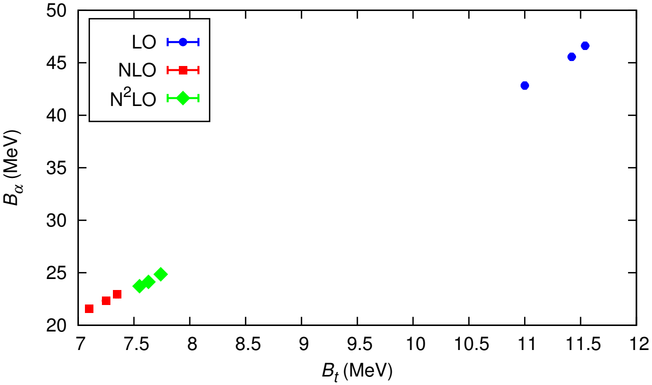

Figure 10: The Tjon line using our results at different chiral orders and cutoff values.

Results

$A = 3$ radii - $r_{\text{pt.}}^2 = r_{\text{ch.}}^2 - r_p^2 - \frac{N}{Z} r_n^2$

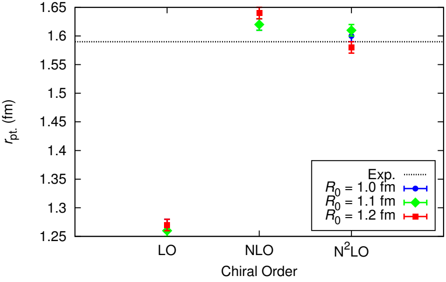

Figure 11: ^{3}H radii at different chiral orders and cutoff values.

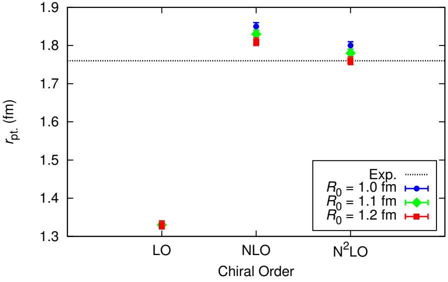

Figure 12: ^{3}He radii at different chiral orders and cutoff values.

Results

^{4}He radii - $r_{\text{pt.}}^2 = r_{\text{ch.}}^2 - r_p^2 - \frac{N}{Z} r_n^2$

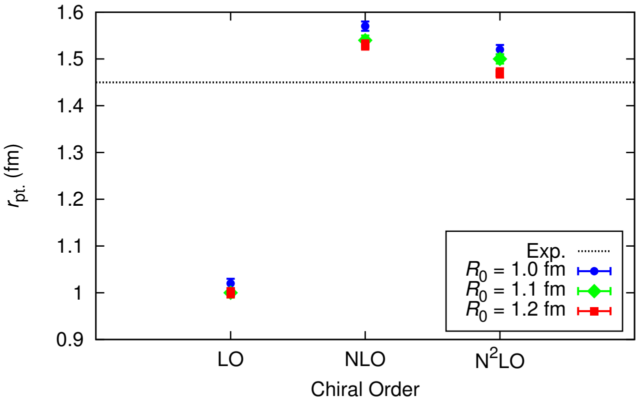

Figure 13: ^{4}He radii at different chiral orders and cutoff values.

Results

^{4}He perturbation - $\langle \Psi_{\mathrm{NLO}} | H_{\mathrm{N^2LO}} | \Psi_{\mathrm{NLO}} \rangle$

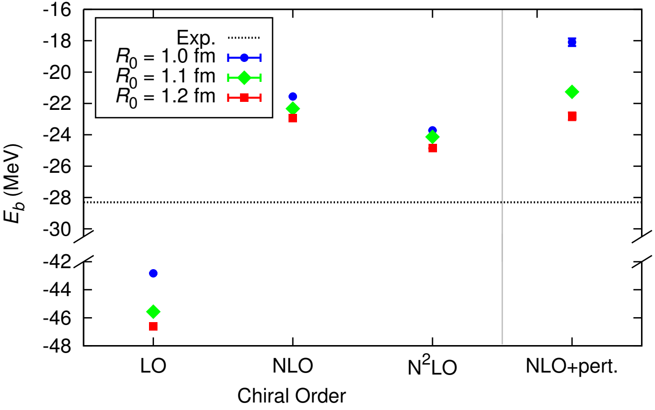

Figure 14: ^{4}He binding energy at different chiral orders and cutoff values plus a first-order perturbative calculation of $\langle H_{\mathrm{N^2LO}} \rangle$.

Hints from the deuteron.

- Write $H \to \langle k' J M_J L' S | H | k J M_J L S \rangle$.
- Diagonalize$\to \{\psi_D^{(i)}(r)\}$.
- Second- and third-order perturbation calculations possible.

Table 1: Perturbation calculations for ^{2}H with different cutoff values for R_0.

Calculation	E_b (MeV)		
	$R_0 = 1.0$ fm	$R_0 = 1.1$ fm	$R_0 = 1.2$ fm
$E^{(0)}_{0\,(\mathrm{NLO})}$	-2.15	-2.16	-2.16
$E^{(0)}_{0\,(\mathrm{NLO})} + V^{(1)}_{\mathrm{pert.}}$	-1.44	-1.80	-1.90
$E^{(0)}_{0\,(\mathrm{NLO})} + V^{(2)}_{\mathrm{pert.}}$	-2.11	-2.17	-2.18
$E^{(0)}_{0\,(\mathrm{NLO})} + V^{(3)}_{\mathrm{pert.}}$	-2.13	-2.18	-2.19
$E^{(0)}_{0\,(\mathrm{N^2LO})}$	-2.21	-2.21	-2.20

Proton distribution: $\rho_{1,p}(r) = \frac{1}{4\pi r^2} \langle\Psi| \sum_i \frac{1+\tau_z(i)}{2} \delta(r - |\mathbf{r}_i - \mathbf{R}_{\text{c.m.}}|)|\Psi\rangle.$

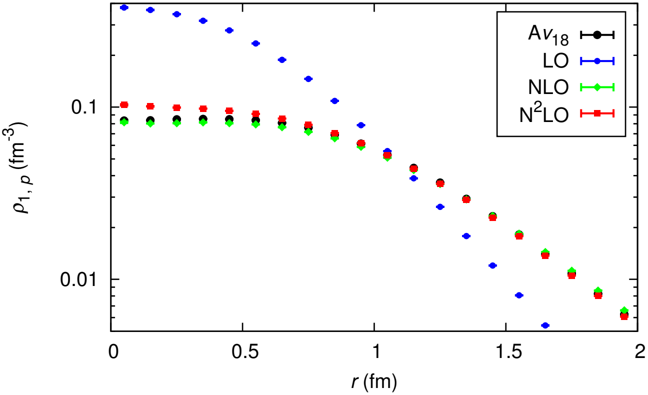

Figure 15: ^{4}He proton distribution at different chiral orders.

Two-body $T = 1$ distribution:

$$\rho_{2,T=1}(r) = \frac{1}{4\pi r^2} \langle \Psi | \sum_{i<j} \frac{3+\boldsymbol{\tau}_i \cdot \boldsymbol{\tau}_j}{4} \delta(r - |\mathbf{r}_{ij}|) | \Psi \rangle.$$

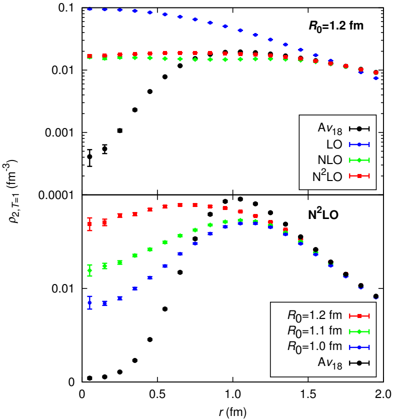

Figure 16: ^{4}He two-body $T = 1$ distributions.

$$\text{Coulomb Sum Rule: } S_L(q) = 1 + \rho_{LL}(q) - Z|F_L(q)|^2;$$
$$\rho_{LL}(q) \propto \int d^3r j_0(qr)\rho_{2,T=1}(r).$$

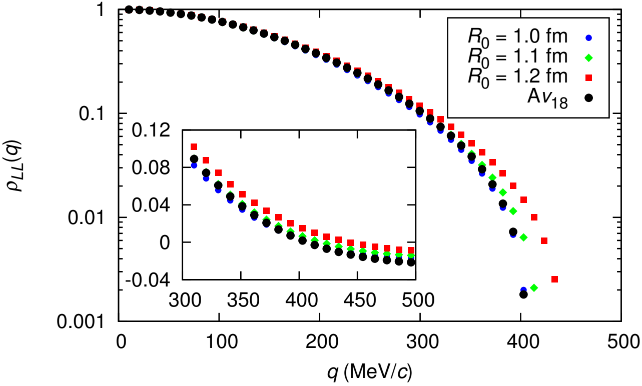

Figure 17: (PRELIMINARY) Fourier transform of the two-body distributions.

- Nuclear structure calculations probe nuclear Hamiltonians.
  - Phenomenological potentials have been very successful but are perhaps unsatisfactory.
  - Chiral EFT potentials have a more direct connection to QCD, but until now, have been non-local.
- GFMC calculations of light nuclei are now possible with chiral EFT interactions.
- Binding energies at $\mathrm{N}^2\mathrm{LO}$ are reasonably similar to results for two-body-only phenomenological potentials.
- Radii show expected trends.
- The softest of the potentials with $R_0 = 1.2$ fm display perturbative behavior in the difference between $\mathrm{N}^2\mathrm{LO}$ and NLO.
- The high-momentum (short-range) behavior of chiral EFT interactions is distinct from the phenomenological interactions.

Conclusion

Future work

- Include 3-nucleon force which appears at N^2LO.
- Include 2-nucleon force at N^3LO (which will be non-local).
- Extend to larger nuclei with $4 < A \leq 12$.
- Second-order perturbation calculation in GFMC.
- Study of, for example, Coulomb sum rule to probe possible consequences of different short-range behavior.

Thank you to my collaborators.
A. Gezerlis, S. Gandolfi, J. Carlson, A. Schwenk, and E. Epelbaum.

Nuclear Computational Low-Energy Initiative